A LUT Baseband Digital Pre-Distorter For Linearization

*Feng Li, *§Bruno Feuvrie, *Yide Wang, *§Anne-Sophie Descamps
*L'UNAM Université - Université de Nantes, UMR CNRS 6164 Institut d'Electronique et de Télécommunications de Rennes (IETR), Ecole polytechnique de l'université de Nantes, Rue Christian Pauc - La Chantrerie BP 50609, 44306 Nantes Cedex 3 France
§IUT GEII Nantes - Site Fleuriaye, Av. du Prof J. Rouxel, 44475 Carquefou, France
feng.li@etu.univ-nantes.fr;
Bruno.Feuvrie@univ-nantes.fr;
Yide.Wang@univ-nantes.fr;
Anne-Sophie.Bacquet@univ-nantes.fr

***Abstract*—This paper proposes a Look-Up-Table Digital Pre-Distorter (LUT DPD) for PA linearization with baseband predistorting procedure. Memory effect can be compensated with Memory Polynomial (MP) modelisation for the wideband applications. Measurements are realized on a PA ZFL-2500 driven by a modulated 16QAM signal with 3.84MHz bandwidth at the carrier frequency of 1.8GHz. The proposed solution achieves maximum ACPR reduction of 12.5dB and EVM correction of 3%.**

Keywords-power amplifier; baseband predistortion procedure; nonlinear memory effect; digital predistortion; linearization.

I. INTRODUCTION

Modern wireless communication systems aim to provide sevices of high data rates for the applications such as video conference, broadcast TV. Constrained by the limited radio frequence resource, spectrally efficient modulation schemes (OFDM, etc.) are widely used in order to increase system capacity. Unfortunately, the resulted non-constant-envelope signals with high Peak-to-Average Power Ratio (PAPR) become more sensitive to the inherent nonlinearity of Power Amplifier (PA) [3]. Thus, a tradeoff between spectrum efficiency and power efficiency must be made. The memory effect increases the distortions on the output signal. The origins of memory effect can be thermal or electrical. Electrical origin is mainly caused by the mismatch of circuit impendence, due to capacitors and resistances. The thermal origin due to the temperature variation may affect low modulation frequencies up to a few megahertz. Therefore, the nonlinear memory effect is device dependant (bias condition, temperature, et) and signal dependant (signal's PAPR, average power, bandwidth, etc).

Digital Pre-Distortion (DPD) is one of the promising techniques for minimizing these distortions. Its advantages lie in the fact that it is reconfigurable and doesn't require deep knowledge of PA's physic circuits [1]. In order to define the predistorting procedure, we need to find a precise model to exactly describe the nonlinear memory effect behavior of the PA.

Figure 1 illustrates the basic principle of DPD. A digital predistortion circuit is inserted before the PA. Then, the overall system produces linearized characteristic. The objective is to efficiently determine the predistorted signal $e(nT)$, which is also the new input of the PA. With ideal linearization, the output of the DPD-PA cascade $S(nT)$ can be written as:

$$S(nT) = G(F(x(nT))) = G_0 x(nT) \quad (1)$$

where $x(nT)$ is the input signal; G represents the nonlinear behavior of the PA, F the behavior of the DPD, which is also the inversed characteristic of G; G_0 is the desired linear gain.

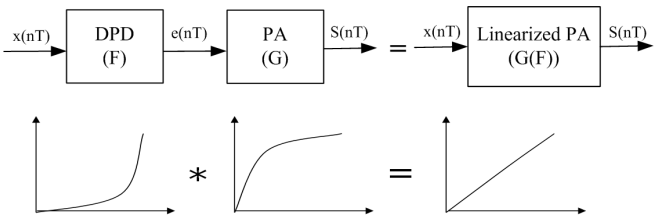

Figure 1. DPD principle

In [5], a baseband DPD based on the Hammerstein model is proposed to linearize the PAs. However this DPD presents two disadvantages. Firstly, the Hammerstein model implicitly separates the memory effect from the nonlinearity. I practice these two effects are often closely related. Secondly, the complex root-finding procedure for finding the amplitude of predistorted signal is not adaptive for the real-time systems. In this paper, we use the MP model to better model the nonlinear memory effect behavior of the PAs and a LUT technique is proposed to avoid the complex root-finding procedure. In section II, the principle of baseband DPD is presented. Based on the baseband signal processing, in section III, the modelisation and the LUT technique are illustrated in detail. In section IV, the measurement is shown. Finally the conclusions and the perspectives are presented.

 ISBN: 978-1-61208-193-9

II. PRINCIPLE OF BASEBAND DPD

Predistorting procedure can be classified into three categories: baseband, Intermediate Frequency (IF) and Radio Frequency (RF). RF predistorter suffers from constrained adaptivity to the variable PA characteristics, due to its high frequency (considered from 800MHz to several GHz for radio communication systems). For IF predistorter, the development of Digital Signal Processing (DSP) still cannot sustain the high sampling frequency to digitize the IF signals. Furthermore, higher power consumption is required for RF/IF predistorters than the baseband predistorters. This affects the flexibility, the size, the mobility, the cost, and the communication quality [2].

Table I
BANDWIDTH FOR DIFFERENT STANDARDS

Standards	Bandwidth
Digital Advanced Mobile Phone System	25kHz
Global System for Mobile Communications	200kHz
Interim Standard 95	1.25MHz
Universal Mobile Telecommunications System	5MHz
Digital Video Broadcasting - Terrestrial	8MHz
3GPP Long Term Evolution and WiMAX	Up to 20MHz
802.11a/g	25MHz
Emerging 4G systems	up to 100MHz

Compared with RF/IF predistorters, baseband DPD presents higher adaptivity to these various parameters. DPD is a DSP-based PD technique. Benefiting from the development of DSP technology, DPD can theoretically to process signal bandwidth greater than 1GHz. But in practice, it is constrained to less than 100MHz [6] for complexity and cost reasons. Baseband predistorting procedure operates on the input signals in baseband frequency, where it is much easier to construct the inversed characteristics [4]. Bandwidths for typical standards are illustrated in Table I. This technique can be applied to different standards and further developed to emerging 4G systems. DPD is added in the stage prior to the DAC and the up-conversion before the PA.

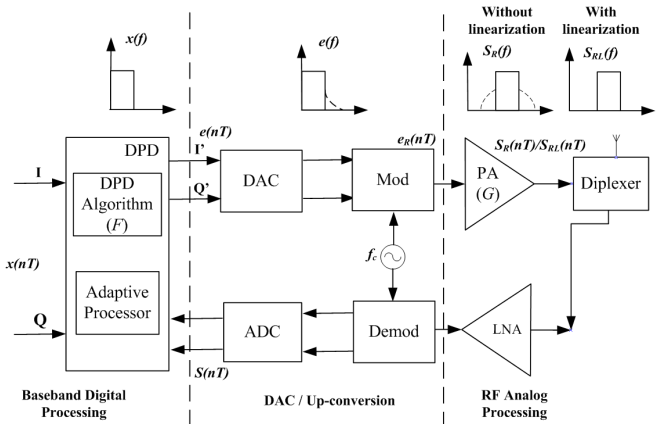

Figure 2. Baseband DPD System Design

Figure 2 presents the typical baseband DPD system design. For the nonlinear system, the gain of the PA G presents device-dependant and signal-dependant characteristics, which can be described as:

$$G = G(B, |x(nT)|, f_c, T \dots) \tag{2}$$

here B is the bandwidth of input signal $x(nT)$, f_c illustrates the carrier frequency, T represents the temperature.

The nonlinear RF output of PA $S_R(nT)$ is down converted to baseband $S(nT)$ to be compared with the baseband input $x(nT)$ and to obtain the inversed nonlinear behavior of PA F:

$$F = \frac{G^{-1}}{G_0} \tag{3}$$

In order to compensate the nonlinear memory effect in wideband systems, the baseband input sample $x(nT)$ is predistorted in DPD (Figure 1):

$$e(nT) = F(x(nT)) \tag{4}$$

The predistorted output signal $e(nT)$ is then directly up converted to RF $e_R(nT)$ (equation (5)) to be amplified by the PA. Finally, the PA's linearized output $S_{RL}(nT)$ (equation (6)) is radiated by the antenna to transmit the messages.

The signal $e_R(nT)$ can be expressed as:

$$\begin{aligned} e_R(nT) =& Re[e(nT)e^{j2\pi f_c nT}] \\ =& I'(nT)\cos(2\pi f_c T) - Q'(nT)\sin(2\pi f_c nT) \end{aligned} \tag{5}$$

The signal $S_{RL}(nT)$ is given by:

$$S_{RL}(nT) = G(e_R(nT)) = G_0 x(nT) e^{j2\pi f_c nT} \tag{6}$$

Note that, with ideal linearization, G_0 is a real constant, presenting no device-dependant or signal-dependant distortions anymore.

As shown in Figure 2, the spectrum of baseband input signal is without spectral regrowth. Due to the nonlinearity or the nonlinear memory effect especially presented by the PA, spectral regrowth appears in the adjacent channels. While with the predistortion, these distortions can be minimized.

III. PROPOSED LUT BASEBAND DPD

A. PA modelisation

The first step in PA linearization is to provide a mathematical description of PA's nonlinear memory effect behavior.

In the narrowband systems, memoryless polynomial model (Figure 3(a)) exhibits good performances in describing the PA's behavior. With the baseband input sample $x(nT)$, the PA's nonlinear output is:

$$S(nT) = a_1 x(nT) + \dots + a_{2j+1} x(nT)|x(nT)|^{2j} + \dots \tag{7}$$

where a_{2j+1} $(j = 0, 1, 2 \dots N)$ are the coefficients of the nonlinearity. N represents the order of nonlinearity.

 ISBN: 978-1-61208-193-9

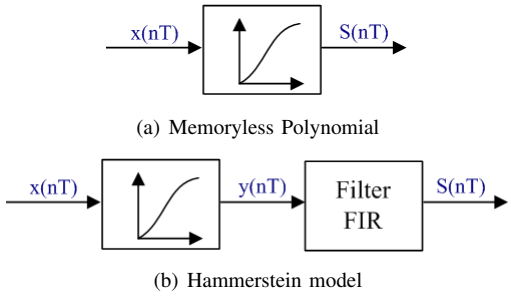

(a) Memoryless Polynomial

(b) Hammerstein model

Figure 3. Model structures

For wideband applications, memory effect should be taken into account. Hammerstein model (Figure 3(b)) consists of a polynomial to model the static nonlinearity and a Finite Impulse Response (FIR) filter to represent the memory effect.

$y(nT)$, the output of the polynomial block is defined as:

$$y(nT) = \sum_{j=0}^{N} b_{2j+1} x(nT)|x(nT)|^{2j} \quad (8)$$

where b_{2j+1} are the coefficients representing nonlinearity.

The output of FIR filter, $S(nT)$, which is also the output of PA is given by:

$$S(nT) = \sum_{i=0}^{P-1} a_i y[(n-i)T] \quad (9)$$

where a_i are the coefficients representing memory effect. P shows the length of memory effect.

The DPD proposed in [5] is based on the Hammerstein model. This model implicitly separates the memory effect from the nonlinearity. However, in practice these two effects are often closely related. In this paper, we use the MP model to better model this nonlinear memory effect behavior. The PA's MP modelisation is given by [7]:

$$S(nT) = \sum_{i=0}^{P-1} \sum_{j=0}^{N} a_{i,2j+1} x[(n-i)T]|x[(n-i)T]|^{2j} \quad (10)$$

where $a_{i,2j+1}$ are the coefficients of the nonlinear memory effect.

B. Look-Up-Table DPD

According to the DPD principle (equation (1)), if the PA is perfectly linearized, we get:

$$\sum_{i=0}^{P-1} \sum_{j=0}^{N} a_{i,2j+1} e[(n-i)T]|e[(n-i)T]|^{2j} = G_0 x(nT) \quad (11)$$

The left member of above equation can be divided into two parts: static nonlinearity $d(nT)$ (equation (12)) and dynamic deviation $P(nT)$ (equation (13)). The first part depends only on the current input at instant nT with $i = 0$. The second part, depending on the previous inputs, is composed of the terms with i varying from 1 to $P-1$.

$$d(nT) = \sum_{j=0}^{N} a_{0,2j+1} e(nT)|e(nT)|^{2j} \quad (12)$$

$$P(nT) = \sum_{i=1}^{P-1} \sum_{j=0}^{N} a_{i,2j+1} e[(n-i)T]|e[(n-i)T]|^{2j} \quad (13)$$

Seperating the static nonlinearity $d(nT)$ and dynamic deviation $P(nT)$, we get:

$$\sum_{j=0}^{N} a_{0,2j+1} e(nT)|e(nT)|^{2j} = G_0 x(nT) - P(nT) \quad (14)$$

With $P(nT)$ being known at instant nT, the corresponding predistorted signal $e(nT)$ can be found for each $x(nT)$. Taking the absolute value of each side of equation (14), we obtain:

$$|\sum_{j=0}^{N} a_{0,2j+1} e(nT)|e(nT)|^{2j}| = |G_0 x(nT) - P(nT)| \quad (15)$$

In [5], the Hammerstein DPD adopts a complex root-finding procedure to calculate the amplitude of the predistorted signal $|e(nT)|$. Unfortunately, this procedure is too time-consuming to be applicable in the real-time applications. In this paper, the LUT principle [7] is proposed to efficiently find $E(m)$, which is also defined as $|e(nT)|$.

Firstly, we decompose the maximum dynamic range of $|e(nT)|$, function of the input amplitude of saturation point and the maximum magnitude of input signal, into M (table size) intervals of equal length. Each interval corresponds to a quantified value $E(m)$ $(m = 1, 2, M)$. Each $E(m)$ corresponds to a value $f(m)$, according to the left member of equation (15). Thus a LUT (TABLE II) is generated according to the following equation:

$$LUT : f(m) = |\sum_{j=0}^{N} a_{0,2j+1} E(m)^{2j+1}| \quad (16)$$

Table II
LUT

INLUT	OUTLUT
$E(1)$	$f(1)$
...	...
$E(m)$	$f(m)$
...	...
$E(M)$	$f(M)$

For each baseband input sample $x(nT)$, we calculate the right member of equation (15) ($|G_0 x(nT) - P(nT)|$) and compare with the values $f(m)$ in the MP LUT to find the corresponding $E(m)$, which is also the desired $|e(nT)|$.

 ISBN: 978-1-61208-193-9

The corresponding phase $Arg(e(nT))$ is calculated by:

$$Arg(e(nT)) = arg\left\{\frac{G_0 x(nT) - P(nT)}{\sum_{j=0}^{N} a_{0,2j+1}|e(nT)|^{2j+1}}\right\} \quad (17)$$

Finally, the predistorted signal $e(nT)$ is given by:

$$e(nT) = |e(nT)|e^{jArg(e(nT))} \quad (18)$$

Table III
LUT DPD ALGORITHM

Initialization:

$$n = 0, P(0) = 0$$

Generate LUT:

$$f(m) = |\sum_{j=0}^{N} a_{0,2j+1} E(m)^{2j+1}|$$

Loop($n = n + 1$)
{
- Calculate:

$$|G_0 x(nT) - P(nT)|$$

- Compare with values OUTLUT in the table to find the corresponding $|e(nT)|$ for each x(nT)
- Calculate:

$$Arg(e(nT)) = arg\left\{\frac{G_0 x(nT) - P(nT)}{\sum_{j=0}^{N} a_{0,2j+1}|e(nT)|^{2j+1}}\right\}$$

- Calculate:

$$e(nT) = |e(nT)|e^{jArg(e(nT))}$$

- Calculate:

$$P[(n+1)T] = \sum_{i=1}^{P-1}\sum_{j=0}^{N} a_{i,2j+1} e[(n+1-i)T]|e[(n+1-i)T]|^{2j}$$

}Goto loop

Table III gives the summary of the proposed LUT algorithm.

The proposed MP model based LUT DPD exhibits lower complexity than the Hammerstein DPD [5]. With the simulation in Matlab, the Hammerstein DPD needs $1.24s$, while only $0.32s$ is required for the LUT DPD with a table size of 1000.

IV. MEASUREMENT

The test bench consists of a Vector Signal Generator (VSG), a Spectrum Analyzer (SA) and a PC. It is designed to be fully automatic by using a Matlab toolbox. The baseband data are generated in Matlab and then sent to the VSG. The VSG (Rhode & Schwartz SMU 200A) receives the complex envelope data via an Ethernet cable (TCP/IP) from the PC and uses a direct up-conversion from baseband to RF. Once the data have been sent to the VSG, the VSG will send the corresponding modulated signal to the PA. The RF input and output signals of the PA are then analyzed by the SA (Agilent E4440A). In this case, the signal analysis software (89601A) provided by this instrument can be used to acquire and demodulate the input and output signals separately. It digitalizes each IF signal by using two ADC ($14bits$), each with a frequency of $100MHz$, totally $200MHz$. These signals are then transferred via an Ethernet cable to the PC, and finally processed in the workspace of Matlab.

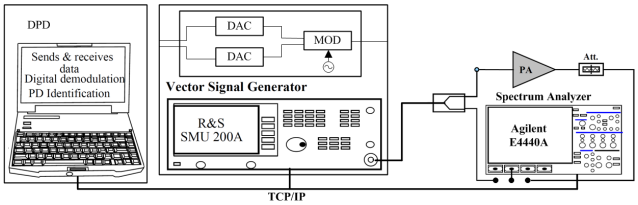

Figure 4. Test Bench

In the PC, the acquired signals by the SA are used to identify the parameters of the PA to obtain the inversed characteristics and then loaded again to the VSG. Finally, the output of the linearized PA is digitized in the SA and sent back to the PC to evaluate the performance of the DPD.

The tested wideband (500-2500 MHz) PA (Mini-Circuits ZFL-2500) has a gain of $28dB(\pm 1.5)$ and the 1dB compression point around the output power of $15dBm$. It is saturated at the average output power around $19.7dBm$. The measurement is driven by a 16QAM modulated signal with $3.84MHz$ bandwidth at the carrier frequency of $1.8GHz$. The offset of adjacent channel is set to be $5MHz$. The pulse shaping filters are square-root raised cosine filters with a roll-off factor of 0.35. A sequence of 200 symbols (4000 samples) is sent to the VSG. The table size is 1000 with N of 4 and P of 2.

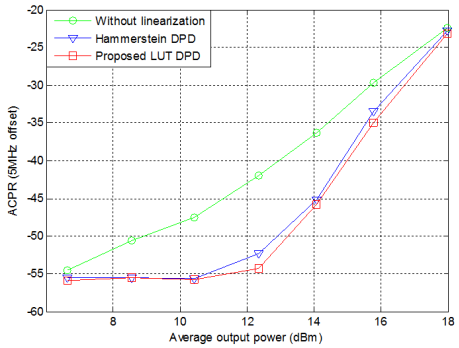

(a) Measured ACPR

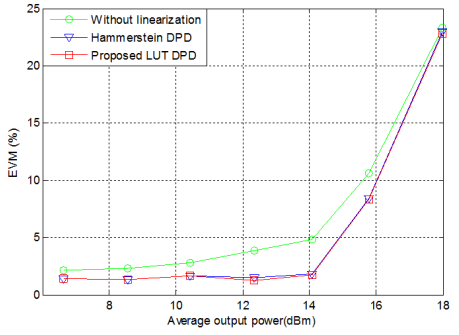

(b) Measured EVM

Figure 5. Measured performances

The measured ACPR performance is presented in Figure

5. The proposed LUT DPD achieves slightly higher ACPR corrections than the Hammerstein DPD, meanwhile with higher simplicity and lower time consumption. The best performance for ACPR reduction is about $12.5dB$ for the proposed LUT DPD and $10dB$ for Hammerstein DPD around the average output power of $12dBm$. For the in-band distortion (EVM), these two DPDs present nearly the same performances with 3% maximum corrections around the average output power of $14dBm$.

V. Conclusion and prospective

In this paper, we proposed a MP model based LUT baseband DPD which presents the ability to linearize the PA with memory effect for the wideband applications. Based on the MP model, a robust modelisation is presented to describe the nonlinear memory effect behavior of the PA. For this DPD, the generated LUT in digital signal processing is used to predistort the baseband signal prior to DAC and up conversion to the desired carrier frequency. The results present maximum ACPR reduction of 12.5dB and EVM correction of 3% with lower complexity compared with the Hammerstein DPD. The LUT is updated continuously so as to enable the DPD to adapt to variations of the transmitter chain characteristics (due to temperature drift, antenna impedances, etc.). We are also planning to consider the nonuniform LUT intervals.

References

[1] F.M. Ghannouchi, and O. Hammi, *Behavioral Modeling and Predistortion*. IEEE Microwave Magazine, Vol. 10, N7, pp. 52-64, Dec 2009.

[2] W.J. Kim, K.J. Cho, S.P. Stapleton, and J.H. Kim, *Baseband Derived RF Digital Predistortion*. Electronics letters, Vol. 42, N8, pp. 468-470, April 2006.

[3] M.A. Hussein, Y. Wang, B. Feuvrie, S. Toutain, and G. Peyresoubes, *Piecewise Complex Circular Approximation of the Inverse Characteristics of Power Amplifiers for Digital Predistortion Techniques*. ICDT '08, pp. 59-63, Bucharest, June 2008.

[4] E. Cottais, and Y. Wang, *Influence of Instruments Bandwidth in the Power Amplifier Linearization Process*. ICDT '08, pp. 11-14, Bucharest, June 2008.

[5] E. Cottais, B. Feuvrie, Y. Wang, and S. Toutain, *Experimental results for power amplifier adaptive baseband predistortion linearization*. IEEE Topical Symposium on Power Amplifiers for Wireless Communications, Long Beach, USA, 8-9, January 2007

[6] A. Katz, R. Gray, and R. Dorval, *Truly wideband linearization*. IEEE Microwave Magazine, Vol. 10, N7, pp. 20-27, Dec 2009.

[7] Li F.; Feuvrie B.; Wang Y.; Chen W.; *MP/LUT baseband digital predistorter for wideband linearization*. Electronics Letters, Vol. 47, N19, pp.1096-1098, September 2011.

 ISBN: 978-1-61208-193-9